remote sensing

MDPI

Article

Derivation of Shortwave Radiometric Adjustments for SNPP and NOAA-20 VIIRS for the NASA MODIS-VIIRS Continuity Cloud Products

Kerry Meyer [1,*], Steven Platnick [1], Robert Holz [2], Steve Dutcher [2], Greg Quinn [2] and Fred Nagle [2]

1 Earth Sciences Division, NASA Goddard Space Flight Center, Greenbelt, MD 20771, USA; steven.platnick@nasa.gov
2 Space Science and Engineering Center, University of Wisconsin, Madison, WI 53706, USA; reholz@ssec.wisc.edu (R.H.); steved@ssec.wisc.edu (S.D.); greg.quinn@ssec.wisc.edu (G.Q.); fred.nagle@ssec.wisc.edu (F.N.)
* Correspondence: kerry.meyer@nasa.gov

Received: 9 November 2020; Accepted: 14 December 2020; Published: 15 December 2020

Abstract: Climate studies, including trend detection and other time series analyses, necessarily require stable, well-characterized and long-term data records. For satellite-based geophysical retrieval datasets, such data records often involve merging the observational records of multiple similar, though not identical, instruments. The National Aeronautics and Space Administration (NASA) cloud mask (CLDMSK) and cloud-top and optical properties (CLDPROP) products are designed to bridge the observational records of the Moderate-resolution Imaging Spectroradiometer (MODIS) onboard NASA's Aqua satellite and the Visible Infrared Imaging Radiometer Suite (VIIRS) onboard the joint NASA/National Oceanic and Atmospheric Administration (NOAA) Suomi National Polar-orbiting Partnership (SNPP) satellite and NOAA's new generation of operational polar-orbiting weather platforms (NOAA-20+). Early implementations of the CLDPROP algorithms on Aqua MODIS and SNPP VIIRS suffered from large intersensor biases in cloud optical properties that were traced back to relative radiometric inconsistency in analogous shortwave channels on both imagers, with VIIRS generally observing brighter top-of-atmosphere spectral reflectance than MODIS (e.g., up to 5% brighter in the 0.67 μm channel). Radiometric adjustment factors for the SNPP and NOAA-20 VIIRS shortwave channels used in the cloud optical property retrievals are derived from an extensive analysis of the overlapping observational records with Aqua MODIS, specifically for homogenous maritime liquid water cloud scenes for which the viewing/solar geometry of MODIS and VIIRS match. Application of these adjustment factors to the VIIRS L1B prior to ingestion into the CLDMSK and CLDPROP algorithms yields improved intersensor agreement, particularly for cloud optical properties.

Keywords: relative radiometry; satellite remote sensing; satellite climate data records; clouds

1. Introduction

The twin Moderate-resolution Imaging Spectroradiometer (MODIS) instruments onboard the National Aeronautics and Space Administration's (NASA) Earth Observing System (EOS) Terra and Aqua satellites to date have provided an extraordinary 20+ (Terra) and 18+ (Aqua) year record of Earth observations that have enabled a broad range of investigations of the Earth's oceans, land and atmosphere [1–4]. For climate applications, however, multidecadal data records that exceed those of the MODIS imagers are necessary to extract meaningful trends and feedbacks. For instance,

given the uncertainties of current satellite imagers, including MODIS, observational records of more than 2–3 decades are required to detect cloud feedbacks [5]. Thus, continuing these satellite geophysical data records beyond MODIS is a desirable goal. To that end, NASA has pursued extending the EOS MODIS geophysical data products to the Visible Infrared Imaging Radiometer Suite (VIIRS) instrument onboard the United States' new generation of polar orbiting weather satellites, beginning with the joint NASA/National Oceanic and Atmospheric Administration (NOAA) Suomi National Polar-orbiting Partnership (SNPP, launched in late 2011) and continuing with NOAA-20 (launched in late 2017) and beyond, with the ultimate goal of obtaining a merged climate data record that provides continuity between the various imagers. VIIRS, similar to MODIS, provides multispectral narrowband observations from the visible (VIS) to the infrared (IR), and the early afternoon equatorial crossing times of SNPP and NOAA-20 (both roughly 13:30 local solar time (LST), though in different orbital planes) are similar to that of Aqua (roughly 13:35 LST).

Among the geophysical data products being extended from MODIS to VIIRS are those specific to clouds, a key component of the Earth's climate system. The EOS standard MODIS cloud mask (MOD/MYD35 for Terra/Aqua, respectively) [6,7] and cloud-top and optical property (MOD/MYD06) [8,9] products were designed for, and have seen widespread use in, process (e.g., [10–12]) and climate (e.g., [13]) studies. While many of the MODIS spectral channels have VIIRS analogs, VIIRS lacks the H_2O and CO_2 IR absorption channels of MODIS that provide information on cloud detection (masking), cloud-top pressure and cloud thermodynamic phase. Therefore, a direct porting to VIIRS of the EOS standard MODIS cloud product algorithms is precluded. Instead, a suite of unified algorithms using only a subset of spectral channels available on both MODIS and VIIRS was pursued, resulting in the cloud mask (CLDMSK) [14] and cloud-top and optical properties (CLDPROP) [15] continuity cloud product algorithms applied to both MODIS Aqua and VIIRS that address the goal of a consistent merged data record via a continuity of approach between the two imagers. Version 1.0 (v1.0) of the CLDMSK product was released for public evaluation in March 2019, while the CLDPROP product has undergone a Version 1.1 (v1.1) reprocessing that was released in November 2019. Note that these initial product releases only include Aqua MODIS and SNPP VIIRS; production of the NOAA-20 VIIRS CLDMSK and CLDPROP products is at present pending ongoing testing.

While the goal of the CLDMSK and CLDPROP algorithms is a continuous imager cloud product data record between MODIS and VIIRS, a number of confounding factors can cause inconsistencies in the respective retrieval products; among these are instrument differences such as pixel size/sampling and shifts in analogous spectral channel locations (e.g., MODIS 2.13 μm vs. VIIRS 2.25 μm that has implications on cloud thermodynamic phase classification and retrievals of effective particle size). For example, assessments of early implementations of the CLDPROP optical property retrievals during algorithm testing revealed large differences between co-located Aqua MODIS and SNPP VIIRS cloud retrievals, notably in liquid phase cloud optical thickness (COT) retrievals for which VIIRS yielded significantly larger COT than MODIS. Figure 1 shows an example of these early results for a scene over the Kamchatka Peninsula on 6 July 2014, which Aqua MODIS (0200 UTC granule) and SNPP VIIRS (0154 and 0200 UTC granules) observed within a few minutes of each other from a nearly coincident ground track. The false color RGBs from MODIS (2.13-0.86-0.66 μm) and VIIRS (2.25-0.87-0.67 μm) are shown in Figure 1a and Figure 1b, respectively. A density plot of co-located liquid phase COT retrievals from MODIS (abscissa) and VIIRS (ordinate), normalized by the maximum bin count and filtered to include only those pixels over ocean for which the view zenith and scattering angle differences between the two imagers are less than 1° (primarily the eastern side of the swath), from an early CLDPROP development test are shown in Figure 1c; the dashed black line denotes the one-to-one line. It is evident that VIIRS retrieves larger COT than does MODIS, a result that cannot be attributed solely to differences in pixel size given the relative homogeneity of many of the clouds in this scene. Rather, an investigation of these COT differences implicated potential differences in radiometry between the two imagers, as SNPP VIIRS appeared to observe brighter spectral reflectance than Aqua MODIS in analogous shortwave channels, in this case the near-IR (NIR) 0.86 μm spectral channel used for COT retrievals

over ocean scenes. This possibility was tested using the MYD06 algorithm by applying a 3% increase in reflectance to the MODIS 0.86 μm channel and comparing the resulting COT retrievals with those using the unaltered reflectance. The results are shown in Figure 1d for the same pixel population shown in Figure 1c. It is clear that even a relatively small 3% radiometric increase in the 0.86 μm channel yields large liquid phase COT retrieval biases comparable to those found between the Aqua MODIS and SNPP VIIRS CLDPROP retrievals.

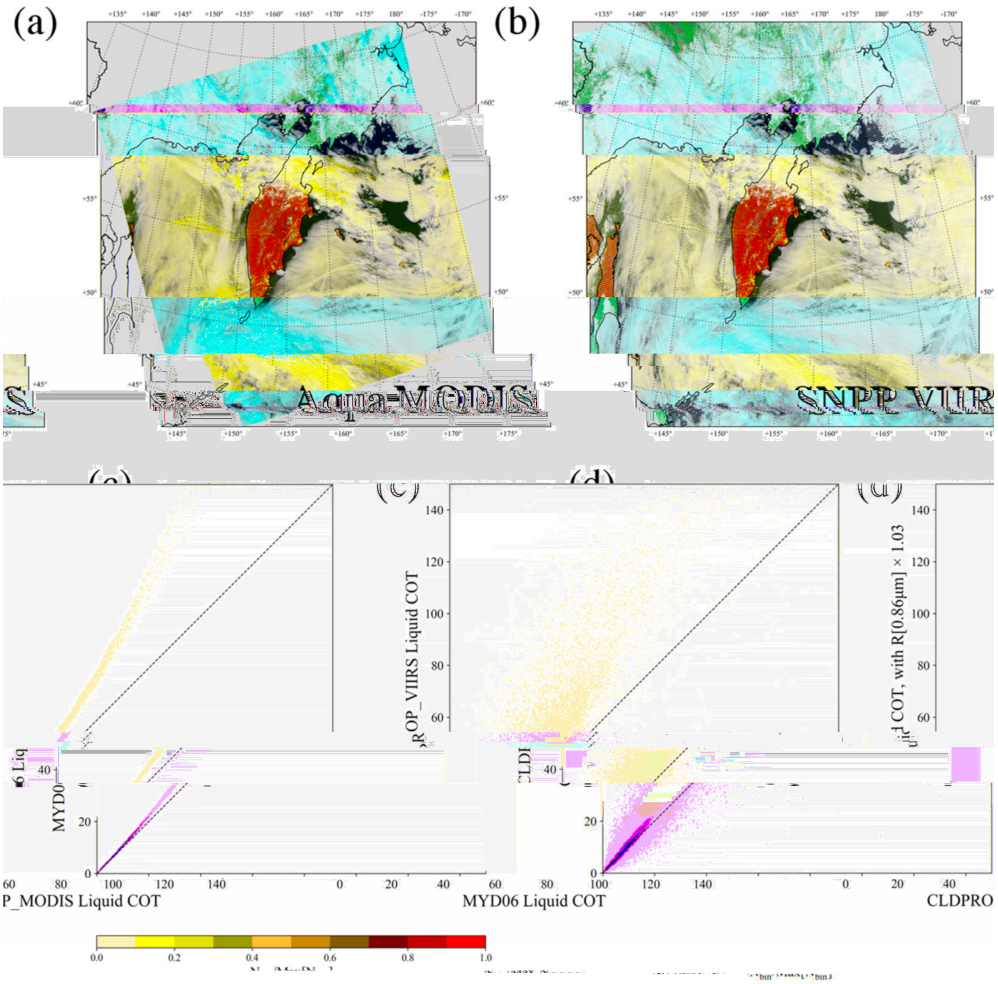

Figure 1. Coincident observations of the Kamchatka Peninsula from Aqua Moderate-resolution Imaging Spectroradiometer (MODIS) (0200 UTC granule) and Suomi National Polar-orbiting Partnership (SNPP) Visible Infrared Imaging Radiometer Suite (VIIRS) (0154 and 0200 UTC granules) on 6 July 2014. (**a**) MODIS false color RGB (MODIS B7-B2-B1). (**b**) VIIRS false color RGB (M11-M7-M5). (**c**) Density plot of co-located MODIS and VIIRS liquid phase cloud optical thickness (COT) retrievals (normalized by the maximum bin count) from an early cloud-top and optical properties (CLDPROP) development test for pixels over the ocean in this scene having intersensor view zenith and scattering angle differences less than 1°. (**d**) Density plot of MYD06 liquid COT for the same pixel population, but with ordinate COT retrieved after increasing MODIS 0.86 μm (B2) reflectance by 3%. The similarity between the two density plots implies that much of the VIIRS COT bias with respect to MODIS is due to a radiometric bias between the two sensors—i.e., VIIRS observes brighter reflectance than MODIS.

The results in Figure 1, however, should not be interpreted as a statement on the absolute calibration of either Aqua MODIS or SNPP VIIRS, nor of the calibration efforts of the MODIS Characterization Support Team (MCST) [16,17] and the combined NOAA/NASA efforts for VIIRS [18,19]. In fact, both instruments are well-characterized in flight using state-of-the-art solar diffuser systems and have known

radiometric errors within specifications. Nevertheless, MODIS and VIIRS each can be calibrated within their respective requirements yet still exhibit relative radiometric differences on the order of those implied in Figure 1. Given that even such small radiometric differences can have impacts on the ability to achieve consistent cloud product retrievals between MODIS and VIIRS, and more generally between any two imager cloud product data records, a suite of tools and analysis infrastructure was developed to assess the radiometric consistency of the SNPP, and later NOAA-20, VIIRS shortwave channels used in the cloud product algorithms with respect to their Aqua MODIS analogs. A subsequent multiyear assessment yielded radiometric adjustment factors for a subset of SNPP and NOAA-20 VIIRS shortwave spectral channels that are applied to VIIRS Level-1b (L1B) calibrated reflectance files prior to ingestion into the CLDMSK and CLDPROP algorithms. Note that Aqua MODIS is used as the reference, not because its better absolute radiometry has been established but because it is the heritage sensor and the anchor of the cloud dataset. This effort, along with a parallel Aqua MODIS-SNPP VIIRS radiometric analysis by the Deep Blue aerosol product (AERDB) team [20], was enabled by significant contributions from the NASA Atmosphere Science Investigator-led Processing System (A-SIPS) at the University of Wisconsin-Madison, the entity responsible for CLDMSK and CLDPROP data production, and included development of intersensor co-located match files and access to extensive computational resources. In this paper, the analysis tools and infrastructure, and their application during the MODIS-VIIRS CLDMSK and CLDPROP cloud product development effort, are discussed in detail. The resulting radiometric adjustment factors for the SNPP and NOAA-20 VIIRS shortwave channels used in the CLDPROP cloud optical property retrievals are then presented, along with examples showing the impact of their implementation, followed by a discussion and conclusions.

2. Materials and Methods

Level-1b pixel-level calibrated reflectance/radiance data from Aqua MODIS and SNPP and NOAA-20 VIIRS, coupled with the EOS Level-2 Aqua MODIS MYD35 cloud mask and MYD06 cloud-top and optical properties products, were used to assess the SNPP and NOAA-20 VIIRS shortwave radiometry relative to Aqua MODIS and to derive radiometric adjustment factors for each. The assessment covers the observational periods of SNPP, beginning March 2012, and NOAA-20, beginning January 2018 through March 2020. Evaluation of the radiometric adjustment factors was performed using the MODIS and VIIRS CLDPROP continuity cloud product algorithms, with the CLDMSK continuity cloud mask serving as input to CLDPROP. Table 1 lists the VIIRS shortwave spectral channels (central wavelengths and sensor band designations) considered in this assessment, along with their MODIS analogs, and identifies their primary uses within the cloud mask and optical property retrieval algorithms. Figure 2 shows the sensor spectral response functions of the channels in Table 1 for Aqua MODIS (blue lines) and SNPP and NOAA-20 VIIRS (solid and dotted red lines, respectively).

Table 1. The SNPP and National Oceanic and Atmospheric Administration (NOAA)-20 VIIRS shortwave spectral channels, and Aqua MODIS analogs, considered in this radiometric assessment. Primary uses within the cloud mask and optical property retrieval algorithms are also listed.

VIIRS Central Wavelength (Band Designation)	MODIS Central Wavelength (Band Designation)	Primary Applications
0.67 μm (M5)	0.66 μm (B1)	cloud detection; cloud optical thickness over land
0.87 μm (M7)	0.86 μm (B2)	cloud detection; cloud optical thickness over water
1.24 μm (M8)	1.24 μm (B5)	cloud optical thickness over snow/ice
1.61 μm (M10)	1.64 μm (B6)	cloud effective radius; cloud thermodynamic phase; cloud optical thickness over snow/ice (coupled with 2.13/2.25 μm)
2.25 μm (M11)	2.13 μm (B7)	cloud effective radius

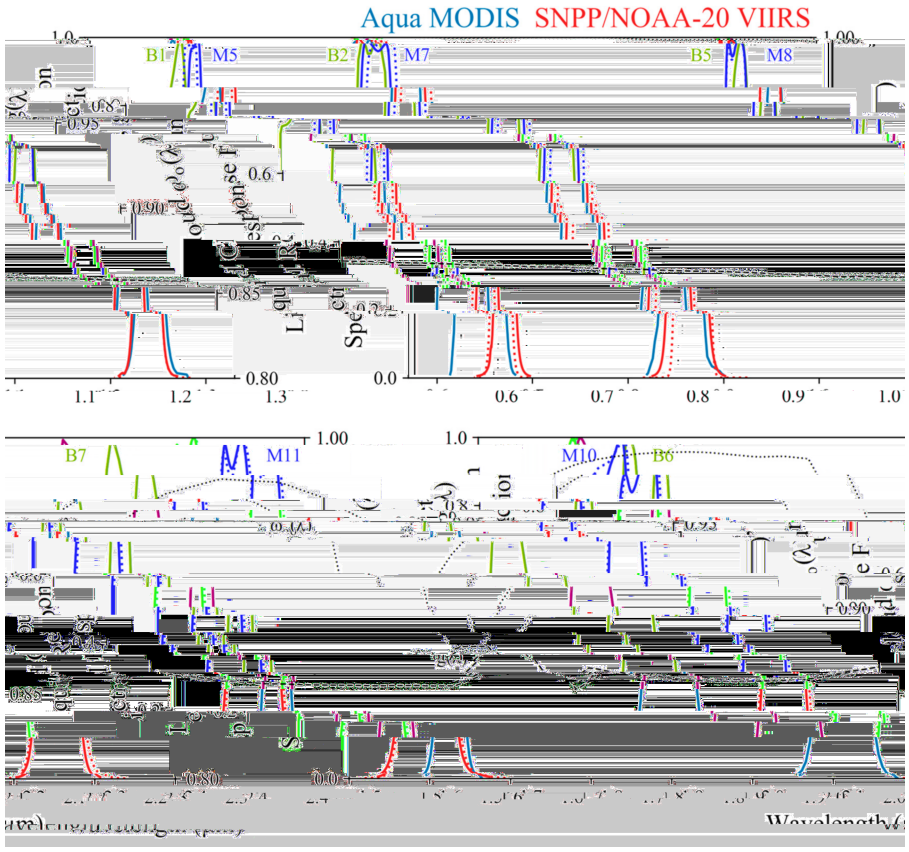

Figure 2. Spectral response functions for the Aqua MODIS (blue lines) and SNPP and NOAA-20 VIIRS (solid and dotted red lines, respectively) channels given in Table 1. The single scattering albedo, $\omega_0(\lambda)$ (dotted black lines), and asymmetry parameter, $g(\lambda)$ (dashed black lines), are also shown for a liquid cloud with effective radius 14 μm.

2.1. Satellite Instruments

2.1.1. Aqua MODIS

The MODIS instrument on NASA's EOS Aqua satellite is a multispectral radiometer that observes reflected solar and emitted thermal radiation from the Earth in 36 narrowband spectral channels from the VIS through the IR (wavelengths roughly between 0.41 and 14.2 μm) [1]. The spatial resolution at nadir varies, with channels 1-2 (central wavelengths of 0.66, 0.86 μm) having 250 m resolution, channels 3–7 (central wavelengths of 0.47, 0.55, 1.24, 1.64, 2.13 μm) having 500 m resolution and the remaining 29 channels having 1 km resolution. While all spectral channel observations were available at their native resolution, the higher resolution channels were also aggregated during ground processing to 1 km resolution and were reported along with the native 1 km channels in the MYD021KM Level-1b product that serves as input to many of the geophysical retrieval algorithms. MODIS observations from each of Aqua's sun-synchronous polar orbits (equatorial crossing time roughly 13:35 LST) were divided into five-minute data granules, for a total of 288 granules per day. With a swath width of 2330 km across track, MODIS observes the entire surface of the Earth in daytime conditions in 1–2 days.

2.1.2. SNPP and NOAA-20 VIIRS

Similar to MODIS, the VIIRS instrument on the NASA/NOAA SNPP satellite and NOAA-20, the first of NOAA's new generation of operational polar-orbiting weather satellite series, is a multispectral narrowband radiometer that observes reflected solar and emitted thermal radiation from the Earth in 16 moderate resolution (750 m at nadir) spectral channels, or M-bands (spanning wavelengths roughly from 0.41 to 12 μm); five imagery resolution (375 m at nadir) spectral channels,

or I-bands (roughly from 0.64 to 11.45 μm); one moderate resolution (750 m at nadir) broad-spectral VIS/NIR day-night band (centered at 0.7 μm). Unlike MODIS, however, VIIRS employs a unique onboard detector aggregation scheme that limits across track pixel growth towards swath edge; for the M-bands, this results in pixel sizes of roughly 1.625 km at the scan edge, vs. MODIS where pixel sizes grow to roughly 2 × 4.9 km (along × across track) at the scan edge [21]. At nadir, VIIRS and MODIS collect 16 (750 m M-band) and 10 (1 km) along track pixels, respectively, with each mirror side scan. However, unlike MODIS, VIIRS employs an onboard bow-tie pixel deletion scheme that removes, from each scan, pixel rows that overlap the preceding and succeeding scans [22]. For the NASA VIIRS data products, VIIRS observations from each sun-synchronous polar orbit (equatorial crossing times roughly 13:30 LST for NOAA-20 and SNPP) are divided into six-minute data granules (note that NOAA divides VIIRS observations differently), for a total of 240 granules per day. With a swath width of 3060 km across track, VIIRS observes the entire surface of the Earth in daytime conditions in only one day.

2.2. Datasets and Algorithms

2.2.1. Geolocation and Calibrated Reflectance Products

Assessing the radiometry of SNPP and NOAA-20 VIIRS with respect to Aqua MODIS requires accurate sensor geolocation and calibrated (by the instrument characterization teams) top-of-atmosphere (TOA) spectral reflectance/radiance. For Aqua MODIS, the pixel-level geolocation (latitude and longitude; solar and viewing zenith and azimuth angles) was provided by the MYD03 product, while the TOA spectral reflectance data were provided by the MYD021KM Level-1b product. Both products were reported at 1 km spatial resolution (at nadir), and from the most recent product releases—Collection 6 (C6) for MYD03 and Collection 6.1 (C6.1) for MYD021KM; C6 MYD021KM was also used in this investigation to demonstrate the impact of calibration changes for one instrument (C6 vs. C6.1 L1B) on the VIIRS relative radiometric adjustment factors. For SNPP and NOAA-20 VIIRS, the NASA-generated datasets for the moderate resolution (750 m at nadir) M-bands were used, namely, VNP02MOD and VJ102MOD, respectively, for spectral TOA reflectance/radiance and VNP03MOD and VJ103MOD, respectively, for geolocation. The SNPP data are Collection Version 1, while the NOAA-20 data are Collection Version 2, though the difference between versions is structural only and not related to the L1B radiometric data itself. Note, however, that intermediate versions of the VNP02MOD and VJ102MOD files were used in the analysis here. Created internally by the U. Wisconsin A-SIPS, these are identical to the original product files but include previously deleted bow-tie pixel observations that were "restored" via nearest-neighbor sampling of the preceding/succeeding scan lines. This intermediate L1B product was also ingested by the CLDMSK and CLDPROP continuity cloud product algorithms. The Aqua MODIS MYD03/MYD021KM and NASA SNPP VIIRS VNP03MOD/VNP02MOD files are publicly archived in the Level-1 and Atmosphere Archive and Distribution System (LAADS) Distributed Active Archive Center (DAAC) housed at NASA Goddard Space Flight Center (GSFC); the NASA NOAA-20 VIIRS VJ103MOD and VJ102MOD products are also archived at the LAADS DAAC.

2.2.2. EOS MODIS Standard Cloud Products

The EOS standard Level-2 Aqua MODIS cloud products consist of the MYD35 cloud mask and the MYD06 cloud-top and optical properties products. MYD35 employs a series of spectral threshold tests that collectively provide a metric that indicates the confidence in a clear sky field of view. The final cloud mask result is defined as one of four confidence levels—namely, confident clear, probably clear, probably cloudy and confident cloudy [23]. Note that the downstream cloud-top and optical properties algorithms designate cloudy pixels specifically as those identified as probably cloudy or confident cloudy by MYD35. MYD06 consists of two distinct products, one providing cloud-top properties and the other cloud optical properties. The MYD06 cloud-top properties algorithm [8] retrieves cloud-top temperature/pressure from either a single channel (i.e., 11 μm) IR-window approach or, in the case of high clouds, a bispectral CO_2-slicing approach using combinations of channels in the 13 μm CO_2

absorption region; also included is an IR-derived cloud thermodynamic phase classification (e.g., ice, liquid). The cloud-top properties are retrieved at the native 1 km resolution and at 5 km resolution using aggregated 1 km IR radiances for improved signal to noise. The MYD06 cloud optical properties algorithm [9] provides an additional thermodynamic phase classification derived from a combination of IR and shortwave-based tests [24]; retrievals of COT and cloud particle effective radius (CER) using the bispectral technique of [25] that typically pairs a nonabsorbing VIS, NIR, or shortwave-IR (SWIR) channel (0.66, 0.86, or 1.24 μm) with an absorbing SWIR (1.64, 2.13 μm) channel or the 3.7 μm midwave-IR (MWIR) channel; water path derived from COT and CER; various quality flags and metrics that include multilayer cloud detection [26], Clear Sky Restoral tests that identify more egregious partly cloudy pixels and enhanced information regarding COT/CER retrieval failures. The MYD35 and MYD06 products, along with their Terra MODIS MOD35 and MOD06 counterparts, are produced by the MODIS Adaptive Processing System (MODAPS) at NASA GSFC and are publicly archived in the LAADS DAAC. For this investigation, the latest release of the EOS MODIS cloud products, Collection 6.1 (C6.1), was used.

2.2.3. NASA MODIS-VIIRS Continuity Cloud Products

Because the H_2O and CO_2 IR absorption channels are extensively used in the EOS MODIS standard cloud product algorithms—primarily in the cloud-top properties algorithm, but also in portions of the cloud mask and optical properties algorithms—the direct porting of these algorithms to VIIRS was not possible. Instead, an approach that uses only a subset of spectral channels common to both MODIS and VIIRS (M-bands only) was pursued, which required a wholesale change of the cloud-top properties algorithm in addition to modifications to the remaining EOS MODIS-heritage algorithms. The CLDMSK cloud mask product algorithm [14] shares direct heritage with MOD35/MYD35, excluding the tests that rely on the H_2O and CO_2 IR absorption channels, and with modifications to various spectral thresholds. The CLDPROP cloud optical property algorithm [15] is a direct porting of MOD06/MYD06, with the exception of the removal of the multilayer cloud detection algorithm and portions of the Clear Sky Restoral algorithm. In addition, updated liquid water complex index of refraction datasets in the SWIR [27] and MWIR [28], measured at a laboratory supercooled temperature of 265K, were used in the forward radiative transfer simulations for the spectral cloud-top reflectance look-up tables (LUTs) [29]; these refractive index datasets provide better consistency between liquid CER retrievals from the MODIS 2.13 μm and VIIRS 2.25 μm spectral channels. The CLDPROP cloud-top properties dataset, on the other hand, replaces the MOD06/MYD06 IR-window and CO_2-slicing algorithms with the NOAA GOES-R Algorithm Working Group (AWG) Cloud Height Algorithm (ACHA) [30], and replaces the IR phase algorithm with the phase algorithm from NOAA's Clouds from AVHRR Extended (CLAVR-x) [31]. The ACHA algorithm employs an optimal estimation framework, retrieving cloud-top height from the 8.6, 10.8, and 12 μm channels using an a priori for high clouds (e.g., cirrus) derived from a Cloud-Aerosol Lidar with Orthogonal Polarization (CALIOP) climatology. The Aqua MODIS and SNPP VIIRS CLDMSK and CLDPROP continuity products are produced by the U. Wisconsin A-SIPS and are publicly archived in the LAADS DAAC at NASA GSFC; the respective NOAA-20 VIIRS products are at present still under evaluation. For this investigation, the latest releases of the CLDMSK and CLDPROP products, v1.0 and v1.1, respectively, were used.

2.2.4. MODIS-VIIRS Co-Located Match Files

Pixel-level co-located match files containing the geolocation and spectral TOA shortwave reflectance and IR radiance of both Aqua MODIS and either SNPP or NOAA-20 VIIRS, in addition to key cloud property datasets from the MYD35 cloud mask and MYD06 cloud-top and optical properties products, were generated by the U. Wisconsin A-SIPS using the spatial co-location methodology described in [32]. These match files, covering the operational periods of SNPP (March 2012 through March 2020) and NOAA-20 (January 2018 through March 2020), enable direct comparisons of MODIS and VIIRS observations. Because MODIS and VIIRS have different pixel spatial resolutions, the coarser

MODIS pixels (1 km at nadir) are considered the "masters", while the VIIRS pixels (750 m at nadir) are considered the "followers", such that more than one VIIRS pixel was co-located with each MODIS pixel. A temporal co-location was also applied by limiting spatial co-locations to scenes having MODIS and VIIRS observation times within 10 min of each other. Further constraints were applied to the pixel co-locations—namely, that the co-located MODIS and VIIRS view zenith and scattering angles must agree within 5° in order to be included in the match files. These temporal and angle matching limitations are intended to mitigate spurious spectral reflectance differences between the two imagers due to temporal changes in meteorology or the angular dependence of scene reflectance, both of which can bias the relative radiometric assessment results. Additional geographical location- and scene-dependent filtering was carried out as described in Section 2.3. The MYD35 and MYD06 datasets in the match files include the final cloud mask results, the 1 km cloud-top pressure retrievals, the optical properties thermodynamic phase classification results, the liquid and ice phase COT and CER retrieved using the VIS/NIR/SWIR and 2.13 μm channel pair, and the atmospherically corrected reflectance for the shortwave channels used in the optical properties retrievals (Table 1). The match file datasets for both SNPP and NOAA-20 VIIRS were archived and are publicly accessible at the U. Wisconsin A-SIPS.

2.3. Derivation of VIIRS Shortwave Radiometric Adjustments

The co-located match files serve as the basis for assessing the shortwave relative radiometric consistency of Aqua MODIS and SNPP and NOAA-20 VIIRS. For this exercise, MODIS was considered the reference imager, with radiometric differences assigned to VIIRS. It is important to emphasize that the choice of MODIS as the reference should not be interpreted as a statement on the absolute calibration accuracy of either imager. Indeed, both imagers are well-characterized yet likely deviate from the truth. MODIS was chosen simply due to its longer heritage and our extensive experience with its characterization.

Returning to Figure 2 and Table 1, note that the central wavelengths and spectral response functions of the analogous MODIS and VIIRS shortwave channels often differ, sometimes quite substantially—e.g., the MODIS 2.13 μm (B7) and VIIRS 2.25 μm (M11) SWIR channels. Because scene TOA reflectance can vary considerably across the shortwave spectrum, such differences in spectral channel placement and sensor response preclude direct radiometric comparisons, even for scenes in the MODIS-VIIRS match files for which co-located observations have been angle-matched in order to mitigate the impacts of the angular dependence of scene reflectance. For instance, the dotted and dashed black lines denote the single scattering albedo, $\omega_0(\lambda)$, and asymmetry parameter, $g(\lambda)$, respectively, of a liquid water cloud particle size distribution having CER = 14 μm. These single scattering properties have strong spectral dependence, particularly for $\omega_0(\lambda)$ in the SWIR (bottom plot) where channel differences are more pronounced. Other phenomena, such as molecular (Rayleigh) scattering, atmospheric water vapor and trace gas absorption and Earth surface reflectance, also have strong spectral dependence that can have disproportionate effects in analogous spectral channels.

The MODIS-VIIRS shortwave radiometric analysis thus necessarily requires the use of forward radiative transfer modeling to account for the above spectral differences. Accordingly, only a subset of MODIS-VIIRS co-locations from the match files in Section 2.2.4 were used—namely, ocean scenes having overcast liquid water clouds, bright scenes for which cloud forward modeling assumptions are thought to be better understood. Co-located scenes were included in this subset only if they met the following criteria:

- Ocean scenes between latitudes 60°S and 60°N;
- Further constrained angle matching was used when creating the match files, such that the co-located view and scattering angles for both imagers must agree to within 1°;
- Liquid phase clouds, determined by the MYD35 cloud mask decision (confident cloudy designation only) and the MYD06 cloud optical properties thermodynamic phase algorithm, with an additional threshold applied to the mean of the "follower" VIIRS 0.87 μm reflectance observations (must be larger than 0.065) within each MODIS pixel (effectively a VIIRS cloud mask);

- Homogeneous MODIS fields of view, where the MYD06 Clear Sky Restoral algorithm (see, e.g., [9]) indicated a likely overcast field of view and the heterogeneity of the co-located "follower" VIIRS pixels, defined by the heterogeneity index $H_\sigma = \frac{stdev[VIIRS\ 0.87\ \mu m\ reflectance]}{mean[VIIRS\ 0.87\ \mu m\ reflectance]}$ [33], must be smaller than 0.1.

Note that the strict homogeneity criterion above was applied in order to mitigate potential subpixel heterogeneity and 3D effects (see, e.g., [34–36]) that may disproportionately affect the coarser-resolution MODIS and thus bias the radiometric comparisons.

A VIIRS spectral radiometric adjustment factor, f_λ, can then be defined for each wavelength λ such that

$$f_\lambda = \frac{R_{\lambda,Exp}}{R_{\lambda,Obs}} \tag{1}$$

where $R_{\lambda,Obs}$ and $R_{\lambda,Exp}$ are the observed and expected VIIRS spectral reflectance, respectively, at the top of the cloud. The VIIRS observed cloud-top reflectance $R_{\lambda,Obs}$ was estimated by atmospherically correcting the VIIRS spectral TOA reflectance, accounting for above-cloud atmospheric gaseous absorption. This was calculated in a manner consistent with the approach of the MYD06 and CLDPROP cloud optical property retrieval algorithms—namely, by scaling the VIIRS observed spectral TOA reflectance by the estimated band-averaged above-cloud two-way path transmittance. The above-cloud transmittance was derived by coupling co-located ancillary atmospheric profiles, taken from the National Centers for Environmental Prediction (NCEP) Global Data Assimilation System (GDAS), with a precomputed transmittance LUT [26] generated from the Moderate Resolution Atmospheric Transmission (MODTRAN) code using an extensive database of cloudy atmospheric profiles from the European Center for Medium-Range Weather Forecasts (ECMWF). This LUT contains two-way path transmittance as a function of viewing and solar zenith angles, cloud-top pressure and column-integrated water vapor amount. Cloud-top pressure was obtained from the co-located MYD06 1 km cloud-top properties retrievals.

Assuming that co-located liquid phase cloud optical property retrievals from MODIS and VIIRS should agree under ideal conditions, the expected VIIRS spectral cloud-top reflectance $R_{\lambda,Exp}$ thus can be estimated from the MODIS COT and CER retrievals via forward radiative transfer calculations. This approach inherently accounts for discrepancies in spectral response functions between analogous MODIS and VIIRS channels, assuming fidelity of the cloud forward model used in the COT and CER retrievals. In practice, the VIIRS CLDPROP precomputed COT-CER retrieval LUTs were searched to find the spectral reflectance that corresponds to the co-located MODIS COT-CER solution, essentially reversing the cloud optical property retrieval inversion process. As described previously (Section 2.2.3), however, the CLDPROP liquid phase optical property retrievals assume an updated liquid water index of refraction measured at 265K which has impacts on CER retrievals from both MODIS and VIIRS. Therefore, the atmospherically corrected reflectance from MYD06 was used to retrieve COT and CER from the CLDPROP MODIS 265K LUTs, from which the expected VIIRS cloud-top reflectance $R_{\lambda,Exp}$ can be inferred from the CLDPROP VIIRS 265K LUTs.

While the radiometric adjustment factors for SNPP and NOAA-20 VIIRS can be calculated at pixel-level directly from the match files using Equation (1), a monthly statistical approach was used instead. In this approach, monthly 2-dimensional (2-D) histograms of VIIRS $R_{\lambda,Exp}$ and $R_{\lambda,Obs}$ for each spectral channel were created for the subset of co-located liquid cloud pixels in the match files meeting the criteria above. A weighted mean spectral radiometric adjustment factor was then defined as

$$f_\lambda = \frac{\sum_{R^*_{\lambda,Exp}} \sum_{R^*_{\lambda,Obs}} f^*_\lambda\left(R^*_{\lambda,Exp}, R^*_{\lambda,Obs}\right) PDF\left(R^*_{\lambda,Exp}, R^*_{\lambda,Obs}\right)}{\sum_{R^*_{\lambda,Exp}} \sum_{R^*_{\lambda,Obs}} PDF\left(R^*_{\lambda,Exp}, R^*_{\lambda,Obs}\right)} \tag{2}$$

where $PDF\left(R^*_{\lambda,Exp}, R^*_{\lambda,Obs}\right)$ is the 2-D histogram of the expected and observed VIIRS spectral reflectance over a given month at each wavelength λ, and $R^*_{\lambda,Exp}$ and $R^*_{\lambda,Obs}$ are the extent of the expected and observed reflectance dimensions, respectively, of the 2-D histogram; f^*_λ is the spectral radiometric adjustment factor at each point in the $R^*_{\lambda,Exp}$ and $R^*_{\lambda,Obs}$ *PDF* space.

Multiyear time series of the monthly spectral adjustment factors from Equation (2) were then used to derive the final radiometric adjustments over the entire observational records of SNPP and NOAA-20 VIIRS. Though these time series enable an assessment of temporal drifts in the relative radiometric differences between Aqua MODIS and SNPP and NOAA-20 VIIRS, for the initial versions of the CLDMSK (v1.0) and CLDPROP (v1.0 and v1.1) products, a single radiometric adjustment for each SNPP and NOAA-20 spectral channel was derived, taken as the respective multiyear time series mean.

An example of the 2-D $R_{\lambda,Exp}$ and $R_{\lambda,Obs}$ histograms, i.e., $PDF\left(R^*_{\lambda,Exp}, R^*_{\lambda,Obs}\right)$, normalized here by the maximum histogram bin value, is shown in Figure 3a for the SNPP VIIRS 0.87 μm channel (M7) for February 2014. A total of 6,325,524 co-locations between Aqua MODIS and SNPP VIIRS met the above filtering criteria for this month and are included in the histogram. The black line indicates the one-to-one line, while the dotted blue line indicates the linear "fit" using the weighted mean radiometric adjustment factor (f_λ in Equation (2)) as the slope. The slope for this spectral channel and month, 0.97 as denoted by the blue text within the plot, indicates that the SNPP VIIRS observations are roughly 3% brighter than expected, at least with respect to the analogous Aqua MODIS spectral channel. The standard error of this slope (radiometric adjustment factor), also denoted in the blue text, is 2.3×10^{-4}, a result that gives confidence in the fit.

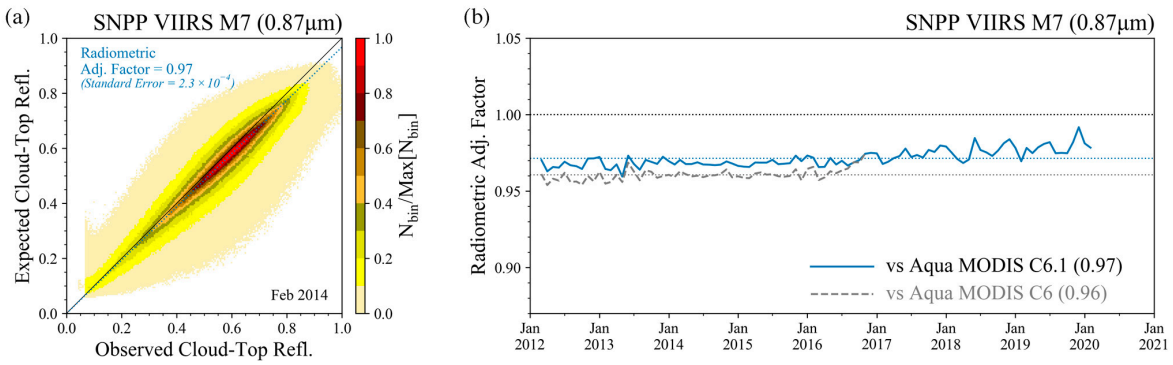

Figure 3. Example shortwave radiometric assessment results for the SNPP VIIRS 0.87 μm channel (M7). (**a**) 2-D histogram of VIIRS expected and observed cloud-top reflectance, normalized by the maximum value in the histogram, for February 2014 (more than 6 million total co-locations with Aqua MODIS). The VIIRS radiometric adjustment factor derived for this month is indicated in the blue text and the slope of the dotted blue line; the standard error of the slope is also denoted. (**b**) Time series of monthly radiometric adjustment factors over the time period considered.

Figure 3b shows the time series of the monthly SNPP VIIRS radiometric adjustment factors for the 0.87 μm channel (M7). Here, the solid blue line denotes the monthly adjustment factors derived using the Aqua MODIS C6.1 L1b as the reference, consistent with the 2-D histogram in Figure 3a. The mean of the time series, used as the final radiometric adjustment factor applied to the SNPP VIIRS L1b prior to CLDMSK and CLDPROP algorithm ingestion, is plotted as the dotted blue line, with its numerical value (0.97) in parentheses in the legend. Two aspects of this time series plot are important to note. First, while the single mean value appears appropriate for much of this time series, a slight trend over the entire observational record shown here is evident, with adjustment factors drifting closer to 1.0 near the end of the record. Second, the dashed gray line, denoting the adjustment factors derived using the earlier Aqua MODIS C6 L1b as the reference, yield different adjustment factors than those derived from the MODIS C6.1 L1b, with a mean value of 0.96. Note that the Aqua MODIS C6.1 L1b reprocessing included updated calibration to mitigate a temporal degradation in a number of the

shortwave channels—namely, a response-vs.-scan (RVS) angle correction [17]. Both the apparent trend and the differences associated with the use of C6.1 vs. C6 Aqua MODIS L1b highlight the fact that drifts or wholesale changes to the calibration of one or both imagers can have impacts on relative radiometry, and thus on the continuity and stability of the merged MODIS-VIIRS climate data record; the implications of this are discussed further in Section 4.

3. Results

Figure 4 shows the time series of monthly SNPP (solid blue line) and NOAA-20 (solid red line) VIIRS radiometric adjustment factors, derived against analogous co-located Aqua MODIS spectral reflectance from the C6.1 L1Bs, for all of the spectral channels listed in Table 1. As in Figure 3b, the dashed gray lines in Figure 4a,b are the derived SNPP VIIRS adjustments against the Aqua MODIS C6 L1B. These C6-derived adjustment factors are only shown for the SNPP VIIRS M5 and M7 channels since the C6.1 RVS correction for Aqua MODIS was applied only to the VIS/NIR channels [17], and C6.1 reprocessing was completed prior to NOAA-20 launch. Note also that the standard errors of the monthly adjustment factors, an example of which is shown for February 2014 in Figure 3b, are not plotted here because their magnitudes (for February 2014, 0.02% of the monthly adjustment factor's value for the 0.87 µm M7 channel) were significantly smaller than the month-to-month variability of the time series. Overall, SNPP VIIRS observed brighter spectral reflectance than would be expected with respect to Aqua MODIS, as indicated by adjustment factors smaller than 1.0, while NOAA-20 VIIRS observed darker spectral reflectance in three of the channels. NOAA-20 VIIRS was also found to be in better agreement with Aqua MODIS, generally within 2%, whereas SNPP VIIRS can be up to 5% brighter than Aqua MODIS (e.g., 0.67 µm (M5)).

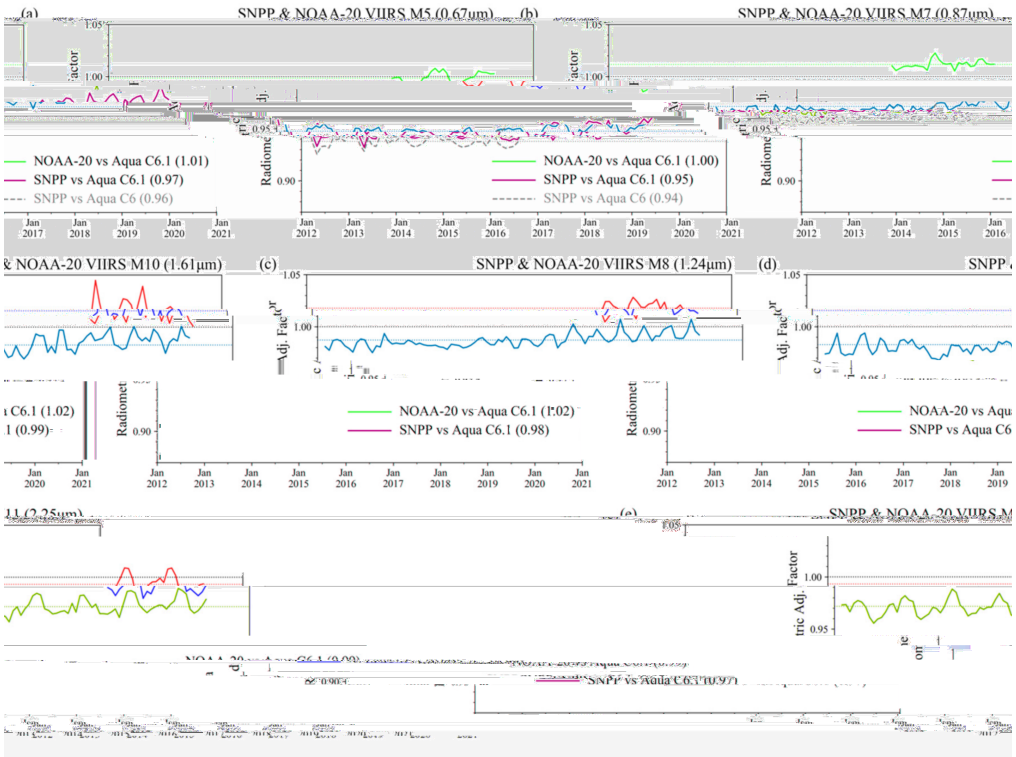

Figure 4. Time series of SNPP (blue lines) and NOAA-20 (red lines) VIIRS spectral radiometric adjustment factors derived for the (**a**) 0.67 (M5), (**b**) 0.87 (M7), (**c**) 1.24 (M8), (**d**) 1.61 (M10) and (**e**) 2.25 µm (M11) channels. The solid blue and dashed gray lines denote SNPP VIIRS adjustment factors derived using Aqua MODIS C6.1 and C6 L1Bs, respectively, as the reference. The thin dotted lines denote the time series means, with exact values indicated in the legends.

Time series means, derived for the time period through March 2020, are indicated in parentheses in the legends of Figure 4 and are summarized in Table 2. The SNPP VIIRS radiometric adjustment (or "gain") factors found by the NASA Deep Blue aerosol product team and applied during processing of the v1.0 AERDB product are also shown in Table 2, for comparison purposes [20]. The Deep Blue adjustments were derived via comparisons with the Aqua MODIS C6 L1B for dark (clear sky) ocean scenes using the same MODIS-VIIRS co-located match files used in the present analysis. Notably, however, the Deep Blue team's analysis only covers the time period through 26 July 2016, and furthermore includes an estimate of the trends in the monthly gain factors for those channels where the gains changed over the time period in question by more than 1% (specifically M7, M8 and M10). Ignoring the trends found by [20], comparing their gains with the spectral adjustment factors derived here from the same Aqua MODIS C6 L1B shows that the two approaches agree well with the exception of the 1.24 (M8) and 2.25 μm (M11) channels, an encouraging result given the focus on different scene types (bright clouds here vs. dark clear sky scenes in [20]). Nevertheless, the application of different spectral adjustment, or gain, factors to the same instrument by different algorithm teams has implications on interproduct consistency, which will be discussed further in Section 4.

Table 2. Shortwave radiometric adjustment factors derived for SNPP and NOAA-20 VIIRS, derived against the Aqua MODIS C6.1 L1B. Adjustment factors derived against the Aqua MODIS C6 L1B following the current approach and those found by [20] are also shown for SNPP VIIRS derived for clear sky ocean scenes for the Deep Blue aerosol product.

	VIIRS Wavelength (Band Designation)		**0.67 μm (M5)**	**0.87 μm (M7)**	**1.24 μm (M8)**	**1.61 μm (M10)**	**2.25 μm (M11)**
Radiometric Adjustment Factor	**NOAA-20**	vs. MODIS C6.1	1.0	1.01	1.02	1.02	0.99
	SNPP	vs. MODIS C6.1	0.95	0.97	0.99	0.98	0.97
		vs. MODIS C6	0.94	0.96	0.98	0.98	0.97
		Deep Blue Gain Factors	0.941	0.963	1.011	0.981	0.931

Figure 5 recreates Figure 1c, a density plot of co-located liquid phase CLDPROP COT retrievals from Aqua MODIS (abscissa) and SNPP VIIRS (ordinate) for the scene in Figure 1a,b, filtered to include only those pixels over ocean for which the view zenith and scattering angle differences between the two imagers are less than 1°. Here, however, the VIIRS COT was retrieved after applying the shortwave spectral radiometric adjustment factors in Table 2 (i.e., those derived for SNPP against Aqua MODIS C6.1), specifically to the 0.87 μm (M7) channel that is used for COT retrievals over ocean surfaces. Comparing this density plot to the one in Figure 1c, it is evident that the COT retrievals are now largely distributed around the one-to-one line (dashed black line), indicating that applying the radiometric adjustment factors to the VIIRS L1B prior to ingestion into the CLDPROP optical properties algorithm has had the desired effect. A similar comparison (not shown) of SNPP VIIRS CLDPROP CER retrievals from the 1.61 and 2.25 μm channels vs. their Aqua MODIS CLDROP analogs (1.64 and 2.13 μm, respectively) before and after application of the respective radiometric adjustment factors reveals little difference. This implies that the impacts of radiometric inconsistency in the SWIR channels were much less significant than in the VIS/NIR, at least for retrievals of the optical properties COT and CER, even though the radiometric adjustments derived for the SNPP VIIRS SWIR channels were similar in magnitude to those in the VIS/NIR (Table 2).

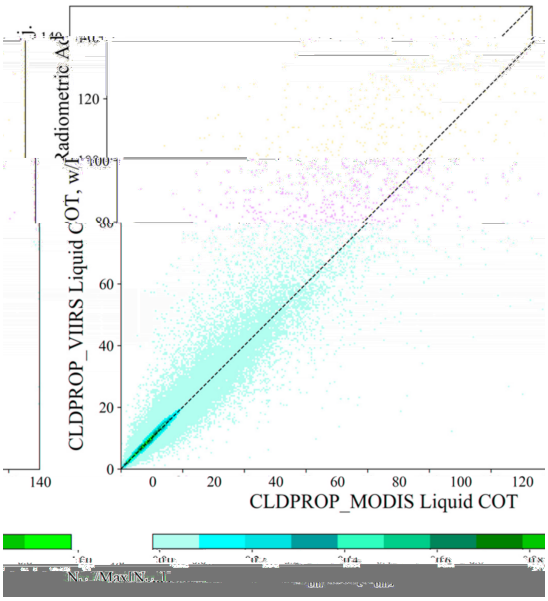

Figure 5. Same as Figure 1c, except for the CLDPROP_VIIRS liquid COT that has been retrieved after applying the SNPP VIIRS radiometric adjustment factors in Table 2.

4. Discussion

Achieving geophysical retrieval continuity across multiple imagers requires a common algorithm approach, analogous instrument capabilities (spectral channel sets, spatial resolution, platform orbital characteristics, etc.) and consistent radiometry; a failure of any leg of this three-legged stool risks failure of the entire continuity project. The SNPP and NOAA-20 VIIRS shortwave radiometric adjustments derived here and shown in Figures 3 and 4 and Table 2, are intended to address one leg—namely, radiometric consistency between VIIRS and Aqua MODIS, specifically for application during processing of the NASA MODIS-VIIRS CLDMSK cloud mask and CLDPROP cloud-top and optical properties continuity products. While these radiometric adjustment factors were derived for the VIIRS imagers, with Aqua MODIS as the reference, in practice any of the three imagers could serve as the reference. Indeed, it is worth reiterating that, even if each of the imagers (Aqua MODIS, SNPP and NOAA-20 VIIRS) is well-characterized and calibrated within mission requirements, the required radiometric accuracy for each nevertheless leaves room for relative radiometric differences that can cause large discrepancies in geophysical retrievals between sensors such as those shown in Figure 1 for Aqua MODIS and SNPP VIIRS COT retrievals. Using Aqua MODIS as the reference was merely a pragmatic choice owing to its being the heritage imager, the anchor of the combined data record and our extensive experience with its calibration and characterization.

The positive impacts of applying the VIIRS shortwave radiometric adjustments in Table 2 are unmistakable, as shown by the improved agreement between Aqua MODIS and SNPP VIIRS COT retrievals in Figure 5. Nonetheless, two results of this investigation have important implications and should be highlighted here. First, while the adjustments (vs. Aqua MODIS C6.1) in Table 2 are the means of the time series in Figure 4, temporal trends are clearly evident—e.g., in the SNPP VIIRS 0.87 μm (M7) channel (Figure 4b), implying calibration drifts in MODIS and/or VIIRS. Second, the differences between the derived SNPP adjustment factors against Aqua MODIS C6.1 and C6 L1B (blue and gray lines, respectively) for the 0.67 (M5) and 0.87 μm (M7) channels (Figure 4a,b, respectively), are due to updates to the Aqua MODIS calibration only. Both of these results highlight the fact that radiometric drifts/trends, or wholesale calibration changes to any of the imagers by their respective characterization teams, can effect changes to intersensor consistency, thus their radiometry relative to each other must be monitored continuously. Given the inherently long timescales involved in developing and vetting formal major calibration updates to the Level-1b products, often several

years or more, the geophysical algorithm teams themselves must play an active role in monitoring relative radiometry and maintain the agility for interim adjustments as needed. Moreover, the trends in Figure 4 for SNPP imply that applying a fixed adjustment factor across the entirety of a mission is likely not an appropriate long-term approach, reiterating the need for continuous monitoring.

Finally, the agreement between the results of this analysis, specifically for SNPP VIIRS against Aqua MODIS C6 L1B, and those of the Deep Blue aerosol team [20] shown in Table 2, are quite encouraging. However, the disagreement for two of the spectral channels (1.24 (M8) and 2.25 μm (M11)) highlights the fact that radiometric consistency between two imagers is difficult to define given the disparate needs of different algorithm teams—e.g., use of dark vs. bright scenes. Therefore, regardless of the best efforts of the respective instrument characterization teams towards intersensor radiometric consistency, the individual geophysical algorithm teams must continuously monitor all instruments and apply adjustments that are appropriate for their application as they see fit. For the CLDMSK and CLDPROP products, the adjustments shown in Table 2 and applied to the VIIRS L1B are also reported in the product metadata to inform the users and facilitate comparisons with other approaches.

5. Conclusions

Early implementations of the NASA CLDPROP cloud optical properties algorithm, a common algorithm designed to extend the EOS MODIS climate data record for clouds to VIIRS on SNPP and NOAA-20+, yielded large differences, particularly in liquid phase COT, between Aqua MODIS and SNPP VIIRS. These differences strongly implied a radiometric bias in one or both instruments. An extensive assessment of the intersensor relative radiometric consistency between Aqua MODIS, used as the reference imager, and SNPP and NOAA-20 VIIRS analogous shortwave channels, was thus pursued.

It was found that, for the versions of the respective L1Bs used here, SNPP VIIRS generally observes brighter shortwave spectral reflectance than should be expected with respect to Aqua MODIS (up to 5% brighter in the VIIRS 0.67 μm (M5) channel), while NOAA-20 VIIRS generally observes darker spectral reflectance (up to only 2% darker in the VIIRS 1.24 (M8) and 1.61 μm (M10) channels). Furthermore, NOAA-20 VIIRS exhibits better overall agreement with Aqua MODIS (see Table 2). Radiometric adjustment factors for the SNPP and NOAA-20 VIIRS shortwave channels used in cloud optical property retrievals were derived over each mission; application of these adjustments to SNPP VIIRS are shown to improve comparisons of liquid phase COT retrievals with Aqua MODIS (Figure 5). For SNPP VIIRS, these adjustments were applied to the VIIRS L1B during processing of the initial public releases of the NASA CLDMSK (v1.0) and CLDPROP (v1.1) continuity cloud products; a similar approach will be taken for the NOAA-20 VIIRS CLDMSK and CLDPROP products.

Author Contributions: Conceptualization, K.M.; methodology, K.M. and S.P.; software, K.M., R.H., S.D., G.Q., and F.N.; formal analysis, K.M.; data production assistance, R.H. and S.D.; writing—original draft preparation, K.M.; writing—review and editing, S.P. and R.H.; visualization, K.M.; project administration, K.M. All authors have read and agreed to the published version of the manuscript.

Funding: This research was supported by the NASA Earth Science Division Terra Aqua Suomi NPP 2017 ROSES solicitation (NNH17ZDA001N-TASNPP).

Acknowledgments: We are grateful to the personnel at the NASA Atmosphere Science Investigator-led Processing System (A-SIPS), University of Wisconsin-Madison Space Science and Engineering Center, led by Liam Gumley, for their assistance in creating the co-location tools utilized in this investigation and processing the match files and radiometric analysis software. We are also grateful for numerous fruitful discussions on MODIS-VIIRS radiometric consistency with the aerosol product teams, specifically Andy Sayer (Deep Blue) and Rob Levy (Dark Target), as well as Jack Xiong and the MODIS and VIIRS Characterization and Support Teams.

Conflicts of Interest: The authors declare no conflict of interest.

References

1. Salomonson, V.V.; Barnes, W.L.; Maymon, P.W.; Montgomery, H.E.; Ostrow, H. MODIS—Advanced facility instrument for studies of the earth as a system. *IEEE Trans. Geosci. Remote Sens.* **1989**, *27*, 145–153. [CrossRef]
2. King, M.D.; Kaufman, Y.J.; Menzel, W.P.; Tanré, D. Remote sensing of cloud, aerosol, and water vapor properties from the moderate resolution imaging spectrometer (MODIS). *IEEE Trans. Geosci. Remote Sens.* **1992**, *30*, 2–27. [CrossRef]
3. Esaias, W.E.; Abbott, M.R.; Barton, I.; Brown, O.B.; Campbell, J.W.; Carder, K.L.; Clark, D.K.; Evans, R.H.; Hoge, F.E.; Gordon, H.R.; et al. An overview of MODIS capabilities for ocean science observations. *IEEE Trans. Geosci. Remote Sens.* **1998**, *36*, 1250–1265. [CrossRef]
4. Justice, C.; Townshend, J.R.G.; Vermote, E.; Masuoka, E.; Wolfe, R.E.; Saleous, N.; Roy, D.P.; Morisette, J.T. An overview of MODIS Land data processing and product status. *Remote Sens. Environ.* **2002**, *83*, 3–15. [CrossRef]
5. Wielicki, B.A.; Young, D.F.; Mlynczak, M.G.; Thome, K.J.; Leroy, S.; Corliss, J.; Anderson, J.G.; Ao, C.O.; Bantges, R.; Best, F.; et al. Achieving Climate Change Absolute Accuracy in Orbit. *Bull. Am. Meteorol. Soc.* **2013**, 1520–1539. [CrossRef]
6. Frey, R.A.; Ackerman, S.A.; Liu, Y.; Strabala, K.I.; Zhang, H.; Key, J.R.; Wang, X. Cloud Detection with MODIS. Part I: Improvements in the MODIS Cloud Mask for Collection 5. *J. Atmos. Ocean. Technol.* **2008**, *25*, 1057–1072. [CrossRef]
7. Ackerman, S.A.; Holz, R.E.; Frey, R.; Eloranta, E.W.; Maddux, B.C.; McGill, M. Cloud Detection with MODIS. Part II: Validation. *J. Atmos. Ocean. Technol.* **2008**, *25*, 1073–1086. [CrossRef]
8. Baum, B.A.; Menzel, W.P.; Frey, R.A.; Tobin, D.C.; Holz, R.E.; Ackerman, S.A.; Heidinger, A.K.; Yang, P. MODIS Cloud-Top Property Refinements for Collection 6. *J. Appl. Meteorol. Climatol.* **2012**, *51*, 1145–1163. [CrossRef]
9. Platnick, S.; Meyer, K.G.; King, M.D.; Wind, G.; Amarasinghe, N.; Marchant, B.; Arnold, G.T.; Zhang, Z.; Hubanks, P.A.; Holz, R.E.; et al. The MODIS cloud optical and microphysical products: Collection 6 updates and examples from Terra and Aqua. *IEEE Trans. Geosci. Remote Sens.* **2016**, *55*, 502–525. [CrossRef]
10. Oreopoulos, L.; Platnick, S. Radiative susceptibility of cloudy atmospheres to droplet number perturbations: 2. Global analysis from MODIS. *J. Geophys. Res.* **2008**, *113*, D14S21. [CrossRef]
11. Toll, V.; Christensen, M.; Quaas, J.; Bellouin, N. Weak average liquid-cloud-water response to anthropogenic aerosols. *Nature* **2019**, *572*, 51–55. [CrossRef] [PubMed]
12. McCoy, D.T.; Field, P.; Gordon, H.; Elsaesser, G.S.; Grosvenor, D.P. Untangling causality in midlatitude aerosol & cloud adjustments. *Atmos. Chem. Phys.* **2020**, *20*, 4085–4103. [CrossRef]
13. Yue, Q.; Kahn, B.H.; Fetzer, E.J.; Wong, S.; Frey, R.; Meyer, K.G. On the response of MODIS cloud coverage to global mean surface air temperature. *J. Geophys. Res. Atmos.* **2017**, *122*, 966–979. [CrossRef]
14. Frey, R.A.; Ackerman, S.A.; Holz, R.E.; Dutcher, S.; Griffith, Z. The continuity MODIS-VIIRS cloud mask. *Remote Sens.* **2020**, *12*, 3334. [CrossRef]
15. Platnick, S.; Meyer, K.; Wind, G.; Holz, R. The NASA MODIS-VIIRS continuity cloud optical properties products. *Remote Sens.* **2020**. submitted.
16. Xiong, X.; Angal, A.; Barnes, W.L.; Chen, H.; Chiang, V.; Geng, X.; Li, Y.; Twedt, K.; Wang, Z.; Wilson, T.; et al. Updates of Moderate Resolution Imaging Spectroradiometer on-orbit calibration uncertainty assessments. *J. Appl. Remote Sens.* **2018**, *12*, 1–19. [CrossRef]
17. Xiong, X.; Angal, A.; Twedt, K.A.; Chen, H.; Link, D.; Geng, X.; Aldoretta, E.; Mu, Q. MODIS Reflective Solar Bands On-Orbit Calibration and Performance. *IEEE Trans. Geosci. Remote Sens.* **2019**, *57*, 6355–6371. [CrossRef]
18. Cao, C.; Xiong, J.; Blonski, S.; Liu, Q.; Uprety, S.; Shao, X.; Bai, Y.; Weng, F. Suomi NPP VIIRS sensor data record verification, validation, and long-term performance monitoring. *J. Geophys. Res. Atmos.* **2013**, *118*, 11664–11678. [CrossRef]
19. Xiong, X.; Butler, J.; Chiang, K.; Efremova, B.; Fulbright, J.; Lei, N.; McIntire, J.; Oudrari, H.; Wang, Z.; Wu, A. Assessment of S-NPP VIIRS on-orbit radiometric calibration and performance. *Remote Sens.* **2016**, *8*, 84. [CrossRef]

20. Sayer, A.M.; Hsu, N.C.; Bettenhausen, C.; Holz, R.E.; Lee, J.; Quinn, G.; Veglio, P. Cross-calibration of S-NPP VIIRS moderate-resolution reflective solar bands against MODIS Aqua over dark water scenes. *Atmos. Meas. Tech.* **2017**, *10*, 1425–1444. [CrossRef]
21. Justice, C.; Vermote, E.; Privette, J.; Sei, A. The Evolution of U.S. Moderate Resolution Optical Land Remote Sensing from AVHRR to VIIRS. In *Land Remote Sensing and Global Environmental Change*; Ramachandran, B., Justice, C., Abrams, M., Eds.; Springer: New York, NY, USA, 2011; Volume 11, pp. 781–806.
22. Cao, C.; Xiong, X.; Wolfe, R.; DeLuccia, F.; Liu, Q.; Blonski, S.; Lin, G.; Nishihama, M.; Pogorzala, D.; Oudrari, H.; et al. *Visible Infrared Imaging Radiometer Suite (VIIRS) Sensor Data Record (SDR) User's Guide*; NOAA Technical Report NESDIS 142A.; NOAA: Washington, DC, USA, 2013.
23. Ackerman, S.A.; Frey, R.; Strabala, K.I.; Liu, Y.; Gumley, L.E.; Baum, B.; Menzel, W.P. *Discriminating Clear-Sky from Cloud with MODIS—Algorithm Theoretical Basis Document*; NASA: Washington, DC, USA, 2010.
24. Marchant, B.; Platnick, S.; Meyer, K.; Arnold, G.T.; Riedi, J. MODIS Collection 6 shortwave-derived cloud phase classification algorithm and comparisons with CALIOP. *Atmos. Meas. Tech.* **2016**, *9*, 1587–1599. [CrossRef] [PubMed]
25. Nakajima, T.; King, M.D. Determination of the optical-thickness and effective particle radius of clouds from reflected solar-radiation measurements. Part 1: Theory. *J. Atmos. Sci.* **1990**, *47*, 1878–1893. [CrossRef]
26. Wind, G.; Platnick, S.; King, M.D.; Hubanks, P.A.; Pavolonis, M.J.; Heidinger, A.K.; Yang, P.; Baum, B.A. Multilayer Cloud Detection with the MODIS Near-Infrared Water Vapor Absorption Band. *J. Appl. Meteorol. Climatol.* **2010**, *49*, 2315–2333. [CrossRef]
27. Kou, L.; Labrie, D.; Chylek, P. Refractive-indexes of water and ice in the 0.65- to 2.5-µm spectral range. *Appl. Opt.* **1993**, *32*, 3531–3540. [CrossRef]
28. Wagner, R.; Benz, S.; Möhler, O.; Saathoff, H.; Schnaiter, M.; Schurath, U. Mid-infrared extinction spectra and optical constants of supercooled water droplets. *J. Phys. Chem. A* **2005**, *109*, 7099–7112. [CrossRef]
29. Platnick, S.; Meyer, K.G.; Amarasinghe, N.; Wind, G.; Hubanks, P.A.; Holz, R.E. Sensitivity of Multispectral Imager Liquid Water Cloud Microphysical Retrievals to the Index of Refraction. *Remote Sens.* **2020**, submitted.
30. Heidinger, A.K.; Li, Y. *Enterprise AWG Cloud Height Algorithm (ACHA)*; NOAA NESDIS Center for Satellite Applications and Research: Washington, DC, USA, 2018.
31. Heidinger, A.K.; Foster, M.J.; Walther, A.; Zhao, X.T. The Pathfinder Atmospheres–Extended AVHRR climate dataset. *Bull. Am. Meteorol. Soc.* **2014**, 909–922. [CrossRef]
32. Holz, R.E.; Ackerman, S.A.; Nagle, F.W.; Frey, R.; Dutcher, S.; Kuehn, R.E.; Vaughan, M.A.; Baum, B. Global Moderate Resolution Imaging Spectroradiometer (MODIS) cloud detection and height evaluation using CALIOP. *J. Geophys. Res.* **2008**, *113*. [CrossRef]
33. Liang, L.; Di Girolamo, L.; Platnick, S. View-angle consistency in reflectance, optical thickness and spherical albedo of marine water-clouds over the northeastern Pacific through MISR-MODIS fusion. *Geophys. Res. Lett.* **2009**, *36*. [CrossRef]
34. Marshak, A.; Platnick, S.; Várnai, T.; Wen, G.; Cahalan, R.F. Impact of three-dimensional radiative effects on satellite retrievals of cloud droplet sizes. *J. Geophys. Res.* **2006**, *111*. [CrossRef]
35. Zhang, Z.; Platnick, S. An assessment of differences between cloud effective particle radius retrievals for marine water clouds from three MODIS spectral bands. *J. Geophys. Res.* **2011**, *116*. [CrossRef]
36. Zhang, Z.; Werner, F.; Cho, H.-M.; Wind, G.; Platnick, S.; Ackerman, A.S.; Di Girolamo, L.; Marshak, A.; Meyer, K. A framework based on 2-D Taylor expansion for quantifying the impacts of subpixel reflectance variance and covariance on cloud optical thickness and effective radius retrievals based on the bispectral method. *J. Geophys. Res. Atmos.* **2016**, *121*, 7007–7025. [CrossRef] [PubMed]